Original Article

The Possible Ameliorative Effect of *Echinacea*, Ginger, and Their Combination on Experimentally Induced Diabetic Nephropathy in a Rat Model: Histological and Immunohistochemical Study

Hoda M. Elsayed, Hekmat Osman Abdel-Aziz, Ghada Mohammed Ahmed, Mohamed Arafa Adly[1], Sherine Ahmed Mohammed

Department of Histology, Faculty of Medicine, Sohag University, [1]Department of Zoology, Faculty of Science, Sohag University, Sohag, Egypt

Abstract

Background: Diabetes represents a chronic disease characterized by hyperglycemia. Several changes in the renal functions had been detected in diabetic patients. **Aim of the Work:** This study was conducted to compare the possible ameliorative role of both ginger and *Echinacea* either alone or in combination upon experimentally induced diabetic nephropathy. **Materials and Methods:** Sixty adult male albino rats were used in this study. Rats were divided into three groups. Control (group I) included 20 rats. Diabetic group (group II) included 10 rats. Group III included 30 rats subdivided into three subgroups 10 animals each: Subgroup IIIa diabetic treated with 100 mg/kg *Echinacea* for 30 days. Subgroup IIIb diabetic treated with 400 mg/kg ginger for 30 days orally. Subgroup IIIc diabetic treated with both 100 mg/kg *Echinacea* and 400 mg/kg ginger for 30 days orally. Hemotoxylin and eosin staining, Periodic acid Schiff and Masson trichrome were done. Ultrastructural examination was done. Immunohistochemical markers used were caspase-3 for apoptosis and CD68 for macrophages. Morphometric and statistical analyses were done. **Results:** Diabetes caused a significant increase in collagen fibers in the renal cortex, the caspase-3 expression as well as the number of macrophages. Ultrastructurally, there was an irregularly thickened glomerular basement membrane and effacement of podocytes. Ginger treatment alone or in combination with *Echinacea* exhibited more pronounced improvement of diabetes-induced degenerative changes and a significant decrease in collagen fibers, the caspase-3 expression as well as the number of macrophages compared to *Echinacea* alone. **Conclusion:** Ginger treatment alone or in combination with *Echinacea* exhibited more pronounced improvement in diabetes nephropathy.

Keywords: Caspase-3, DC68, Diabetic nephropathy, *Echinacea*, ginger

Introduction

Diabetes mellitus (DM) is a chronic systemic disorder characterized by hyperglycemia.[1] Diabetes prevalence reached more than 350 million people worldwide.[2]

Diabetic nephropathy (DN) is one of the serious complications of DM. DN leads to chronic renal failure and end-stage renal impairment.[3]

Rodent models provide valuable insight into the mechanism of DN evolution. Moreover, they are helpful in studying how new treatments work.[2] The induction of diabetes model by streptozotocin (STZ) is a commonly used method. STZ is particularly toxic for the β-cells which are the insulin-secreting cells in the islets of Langerhans.[1]

Oxidative stress is the end result of many mechanisms in the evolution of DN including hyperglycemia and inflammation of the kidney oxidative stress has a key role in the development and progression of DN.[4]

Received: 11-07-2022 **Revised:** 30-09-2022
Accepted: 06-10-2022 **Published:** 11-01-2023

Access this article online

Quick Response Code:

Website: http://www.jmau.org/

DOI: 10.4103/jmau.jmau_62_22

Address for correspondence: Dr. Sherine Ahmed Mohammed, Department of Histology, Faculty of Medicine, Sohag University, Sohag, Egypt.
E-mail: loua.sherine@yahoo.com

How to cite this article: Elsayed HM, Abdel-Aziz HO, Ahmed GM, Adly MA, Mohammed SA. The possible ameliorative effect of *Echinacea*, ginger, and their combination on experimentally induced diabetic nephropathy in a rat model: Histological and immunohistochemical study. J Microsc Ultrastruct 2024;12:199-210.

Echinacea purpurea (EP) which is also known as *Asteraceae* is a medical herb. The active components of EP are alkamides, phenols (including derivatives of chicoric acid), and polysaccharides. Polyphenols are considered the most active component of them. They represent secondary metabolites and act as free radical scavengers towards reactive oxygen species. *Echinacea* extracts exhibited anti-oxidative and anti-inflammatory effects. In addition, EP has antibacterial, antiviral, and anticancer properties.[5] The micro-nanoencapsulated EP ethanol extract had an ameliorative effect on the diabetic model.[6] Furthermore, EP ethanol extract alone ameliorated testicular toxicity and reproductive dysfunction in diabetic rat model.[7] Mohammedsaleh and Aljadani[8] reported that EP attenuated diabetic nephrotoxicity in rat model and explained that by hypoglycemic and anti-oxidative effects of the EP.

Ginger, also known as *Zingiber officinale*, belongs to the plant family *Zingiberaceae*. Its typical aroma and flavor make it a famous spice. Moreover, ginger is widely used as traditional Chinese Medical herbs.[9] It was used to treat diverse inflammatory disorders such as stomachache and arthritis.[10] Previous studies reported its role to treat nonalcoholic fatty liver disease.[11] In addition, it was proved to be used in the treatment of chemotherapy-induced dyspnea[12] and primary dysmenorrhea.[13] Ginger had hypoglycemic effect, antioxidant, and regenerative actions on different organs such as the liver and spleen. This role may be due to its primary bioactive components. These components include gingerols, zingerone, shogaols, and paradols.[14]

Al Hroob *et al*.[15] reported that ginger attenuated diabetic nephrotoxicity in rat model due to its hypoglycemic and anti-inflammatory effects. The present study compares the possible ameliorative effects of both EP and ginger alone and in combination on an experimental model of DN.

Materials and Methods

Animals

Sixty adult male albino rats (200–250 g weight), purchased from animal house in Faculty of Science, Sohag University, were used. Animals were allowed for free access to chow and water. The approval of Sohag ethical committee was taken in accordance with the ethical guidelines for experimental animals, code: IRB00013006-10112022, Date 5 January 2021.

Chemicals

The chemicals are summarized in Table 1.[16]

Table 1: Chemicals

Chemicals	Company
Streptozotocin	Purchased from Sigma-Aldrich chemicals company
Ginger powder	
Echinacea purpurea	
Rabbit polyclonal anti-CD68 antibody	E13920, Thermo scientific company, Neomarks, Fremont, USA. Dilution 1:100
Rabbit polyclonal cleaved caspase-3 antibody	RB-1197-P0(Ab4), Thermo scientific company, Neomarks, Fremont, USA. Dilution 1:100

Experimental design

Sixty rats were randomly divided into three experimental groups:

- Group I: Control (normoglycemia group) was subdivided into 4 subgroups 5 animals each as follows: Subgroup Ia: Animals were fed with a regular diet for 60 days. Subgroup Ib received EP daily 100 mg/kg for 30 days orally through gastric gavage. Subgroup Ic: Received ginger extract daily 400 mg/kg for 30 days orally through gastric gavage. Subgroup Id: Received ginger extract daily 400 mg/kg and EP daily 100 mg/kg for 30 days orally through gastric gavage
- Group II: Diabetic group included 10 animals. For induction of diabetes, animals received a single intraperitoneal injection of STZ (60 mg/kg). After 72 h, a tail blood sample from each rat was obtained, and blood glucose levels were determined spectrophotometrically using diagnostic kits, STZ-treated rats which had blood glucose below 300 mg/dl were excluded.[1] After diabetes is well established in rats then they were fed with a regular diet for 30 days
- Group III: Subdivided into three subgroups 10 animals each as follow:
  - Subgroup IIIa: Diabetic animals received EP daily 100 mg/kg for 30 days orally through gastric gavage[17]
  - Subgroup IIIb: Diabetic animals received ginger extract daily 400 mg/kg for 30 days orally through gastric gavage[18]
  - Subgroup IIIc: Diabetic animals received ginger extract daily 400 mg/kg and EP daily 100 mg/kg for 30 days orally through gastric gavage.

At the end of the experiment, the rats were anesthetized by inhalation of diethyl ether. The animals were sacrificed. After dissection of kidneys, specimens were processed for histological (light microscopy and electron microscopic) studies and immunohistochemical staining.

Light microscopy

Kidney specimens were fixed for 24 hours in 10% buffered formalin and processed till paraffin embedding. The blocks were sectioned using (Leica RM 2125) microtome. Sections (5 um thickness) were stained with:

1. Hematoxylin and eosin stain (H and E): General histological stain
2. Masson trichrome stain for collagen fibers
3. Periodic acid–Schiff (PAS) stain: For examination of brush borders and basement membranes.[19]
4. Immunohistochemical study:

For detection of macrophages using CD68 antibody[20] and apoptotic cells using caspase-3 antibody.[21] Deparaffinization, rehydration, and antigen retrieval were carried out then using the avidin-biotin-peroxidase technique. Sections were counterstained with Mayer's hematoxylin, dehydrated, and

cleared.[22] Positive cells for CD68 show brown cytoplasmic staining. Positive cells for caspase-3 appear with brown cytoplasmic staining and may also show nuclear staining. Negative control was done by the omission of primary antibody.

Electron microscopy

Specimens were immediately fixed in 2.5% glutaraldehyde for 2 h at 4°C, postfixed in 1% osmium tetroxide for 1 h at 4°C. The specimens were processed and embedded in resin. Semithin sections (1 μm) were stained by toluidine blue. Ultrathin sections (500–800 nm) counterstained with uranyl acetate and lead citrate were examined with a transmission electron microscope.[23] This technique was done in electron microscopy unit at Assuit University.

Morphometric Studies

Using light microscopy Leica ICC50 Wetzlar (Germany), ten nonoverlapped high power fields (×400) were taken for each section at the Histology Department, Faculty of Medicine, Sohag University. Each field was analyzed using Image J1.51n software (National institutes of health USA Java 1.8.0_66 (32-bit):

1. Collagen area percentage with Masson's trichrome was measured[24]
2. PAS-positive area delineating basement membranes percentage was measured[25]
3. The number of CD68-positive cells was counted[26]
4. The area percentage of caspase-3 expression was measured.[27]

The cleaved caspase-3 positive cells; labeling index (LI) was calculated as: (the number of positive cells/number of total cells counted in the field) × 100.[28]

Statistical analysis

The statistical package SPSS, version 16.0 was used. Data were presented as mean ± standard deviation and the values were considered statistically significant as $P \leq 0.05$. One way ANOVA test was used followed by *post hoc* test to compare the results between groups of the recordings reported by two observers.[29]

Results

Hematoxylin and eosin stain

Examination of kidney sections of all subgroups in group I revealed the same histological findings so all were considered a control group. H and E stained sections of the control group revealed that the renal cortex contains the renal corpuscle and the renal tubules. The renal corpuscle is formed of renal glomeruli which are formed of a tuft of capillaries and surrounded by Bowman's capsule. The latter is formed of parietal and visceral layers. The parietal layer is lined with simple squamous epithelium. The proximal tubules (PT) are lined with cuboidal cells with highly acidophilic cytoplasm. Their nuclei are central rounded and vesicular. The cells have ill-defined boundaries and apical brush borders. The distal tubules (DT) exhibit a wide lumen. They are lined with low cuboidal cells having rounded vesicular nuclei with no apical brush borders [Figure 1a-d]. On the other hand, group II showed a widening of urinary space with congestion of the glomerular capillaries which appeared widely spaced. Most of the PT showed dilated lumen and lost brush borders. Proximal and distal tubular cells had vacuolated cytoplasm and deeply stained pyknotic nuclei as well as intraluminal acidophilic debris representing desquamated cells [Figure 1e]. All group III subgroups [Figure 1f-h] showed improvement in the diabetic histological changes; Subgroups IIIa, IIIb revealed an apparent narrower urinary space with less congested and near to each other glomerular capillaries compared to group II. PT showed partially regular brush borders. Cells of proximal and DTs were less vacuolated compared to diabetic rats. Subgroup IIIc appeared more or less similar to control.

Periodic acid–Schiff technique

Positive PAS reaction was observed in basement membranes of renal corpuscles, glomerular capillaries, and renal tubules of the Control kidney. It also showed a regular brush border of PT. However, the diabetic group II showed an increase in the intensity of PAS reaction with a significant increase in area percentage at the site of basement membranes of renal corpuscle, renal glomeruli, and renal tubules compared to control. The brush borders of the PT appeared irregular and interrupted. All group III subgroups showed decreased intensity of PAS reaction with a significant decrease in area percentage at the site of basement membranes compared to group II with IIIa still significantly higher than control. Subgroups IIIb and IIIc showed a significant decrease versus IIIa and insignificant difference compared to control [Figure 2 and Table 2].

Table 2: Statistical results for means of collagen %, periodic acid-Schiff %, caspase 3%, caspase 3 labeling index, and number of macrophages

	Mean collagen % (±SD)	Mean PAS % (±SD)	Mean caspase 3 percentage % (±SD)	Mean caspase 3 labelling index (±SD)	Mean CD68 positive (cells) (±SD)
Control	11.1128±1.7	3.56±0.4	2.30±0.7	1.60±0.5	2.06±0.8
Group II	31.87±2.04[a]	10.38±1.1[a]	27.45±1.1[a]	27.21±5.1[a]	45.41±4.9[a]
Group IIIa	16.47±1.41[a,#]	6.5479±0.6[a,#]	15.40±1.9[a,#]	17.52±1.1[a,#]	23.70±4.5[a,#]
Group IIIb	14.73±2.10[a,#,*]	3.7139±0.7[#,*]	11.86±2.4[a,#,*]	14.83±0.7[a,#,*]	20.82±2.03[a,#,*]
Group IIIc	14.17±1.92[a,#,*]	3.5045±0.4[#,*]	8.22±1.1[a,#,*,b]	11.17±1.1[a,#,*,b]	17.64±1.45[a,#,*,b]

[a]Significant compared to control, [#]Significant compared to Group II, *Significant compared to Group IIIa, [b]Significant compared to Group IIIb.
PAS: Periodic acid Schiff, SD: Standard deviation

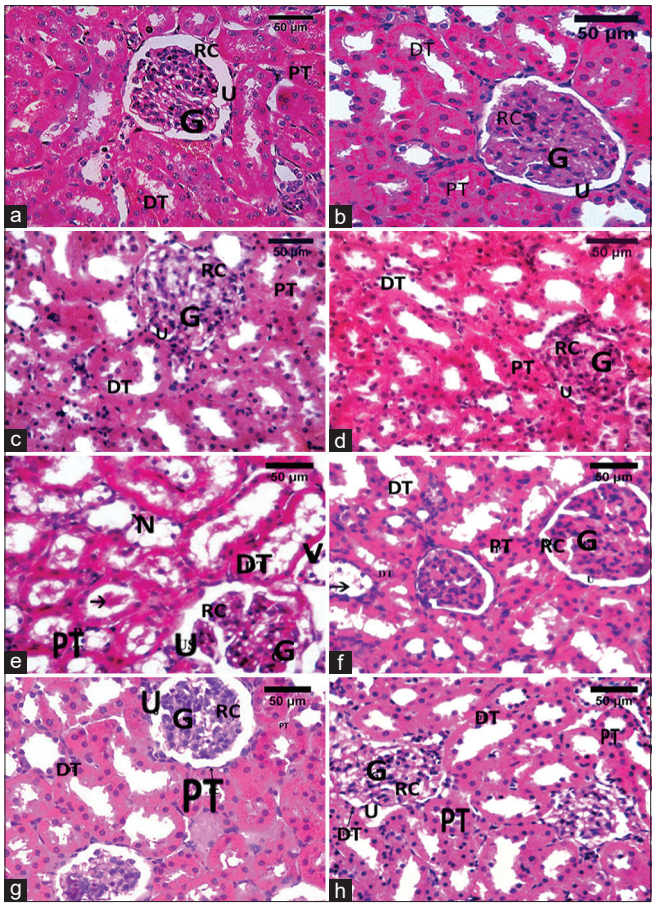

Figure 1: Photomicrographs of kidney sections (a-d) The control subgroups Ia, Ib, Ic, and Id respectively showing the RC glomerular capillaries (G), urinary space (U), PT with narrow lumen and lined with cuboidal cells having apical brush border with vesicular nuclei and acidophilic cytoplasm. DT with a wide lumen and lined with cuboidal cells with vesicular nuclei and acidophilic cytoplasm (e) (group II) showing, the RC glomerular capillaries (G) with mesangial expansion and widening of urinary space (U), vacuoles (V), loss of brush border of PT and pyknotic nuclei (N), DT. Luminal acidophilic debris (arrow). (f) Subgroup IIIa and (g) Subgroup IIIb: Showing decreased degenerative changes (h) Subgroup IIIc is more or less similar to the control; the RC glomerular capillaries (G), urinary space (U), PT DT scale bar = 50 μm (H and E, ×400). RC: Renal corpuscle, PT: Proximal tubule, DT: Distal tubule, U: Urinary space, V: Vacuoles, G: Glomerular capillaries

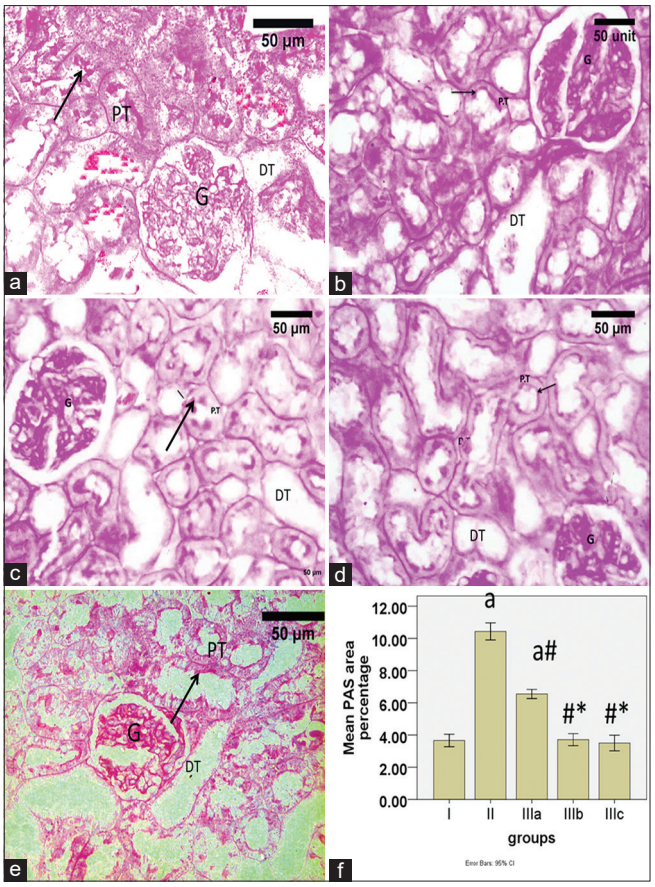

Figure 2: Photomicrographs of kidney sections. (a) Control showing a positive reaction in basement membranes of renal corpuscles, glomerular capillaries (G), renal tubules (PT, DT) and the brush border of PT (arrow). (b) Diabetic rats showing increased intensity of PAS reaction with interrupted brush border (arrow) and thickened Basement membranes of the renal corpuscles, glomerular capillaries (G), renal tubules (PT, DT). (c) Subgroup IIIa and d: Subgroup IIIb: Showing decreased intensity of PAS with partially destructed brush border e: Subgroup IIIc is more or less similar to the control. Renal corpuscles (G), PT, DT, brush border (arrow). Scale bar = 50 μm (PAS, ×400) (f) Histogram showing the mean of PAS basement membranes positive area percentage in all groups. aSignificant compared to control, #Significant compared to group II, *Significant compared to group IIIa. PT: Proximal tubule, DT: Distal tubule, G: Glomerular capillaries, PAS: Periodic acid–Schiff, G: Glomerular capillaries

Masson trichrome stain

There were few collagen fibers around the glomeruli and tubule in the control. In the diabetic group, collagen fibers were present in the renal interstitium and were markedly deposited around the glomeruli and tubules. In all group III subgroups, the area percentage of collagen significantly reduced compared to group II, collagen fibers were seen in the renal interstitium, around the glomeruli and tubules. Group III subgroups were still significantly higher than control with Subgroups IIIb and IIIc showed a significant decrease versus IIIa [Figure 3 and Table 2].

Immunohistochemical results

Caspase-3 antibody

Both cytoplasmic and sometimes nuclear immunoexpression of active caspase 3 were detected in positive cells. The control group showed few caspase-3 positive cells in renal corpuscles and renal tubules. Group II showed an apparent increase in caspase-3 expression compared to control, being demonstrated in renal corpuscles and renal tubules. A significant increase in caspase-3 expression area percentage and LI in group II was detected compared to control. All group III subgroups showed less expression of caspase-3 in renal corpuscles and renal tubules with a significant decrease in caspase-3 expression area percentage and LI versus group II but still significantly higher than control. Subgroups IIIb and IIIc showed a significant decrease versus IIIa. Subgroup IIIc showed a significant decrease compared to IIIb [Figure 4 and Table 2].

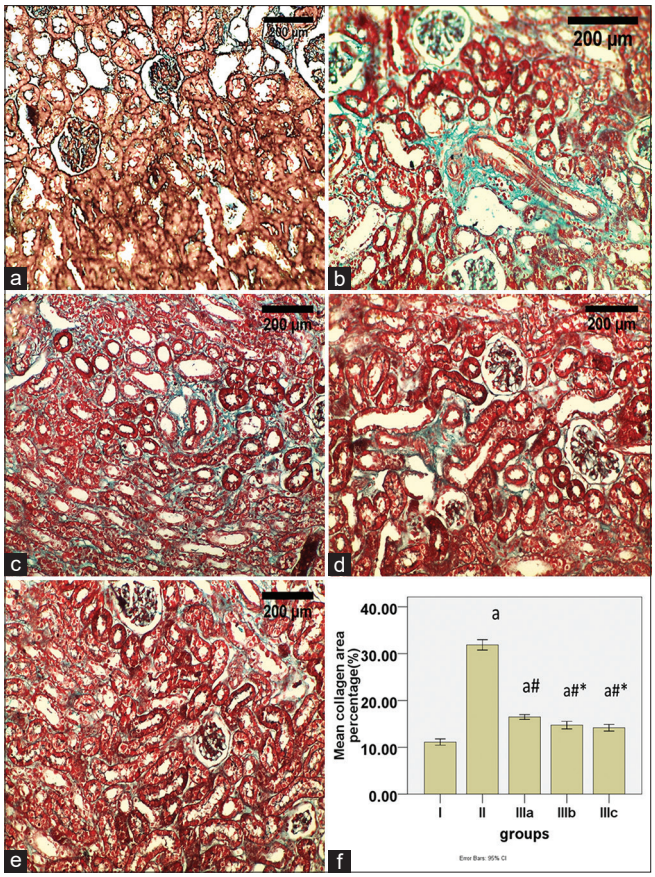

Figure 3: Photomicrographs of kidney sections. (a) Control showing few collagen fibers around the glomeruli and renal tubule (b) Group II showing increased collagen fibers around the glomeruli and tubules and in renal interstitium. (c) Subgroup IIIa, (d) Subgroup IIIb) and (e) Subgroup IIIc: Showing decreased collagen fibers. Scale bar = 50 μm (Masson trichrome, ×400) (f) Histogram showing the mean of collagen area percentage in all groups. aSignificant compared to control, #Significant compared to group II, *Significant compared to group IIIa

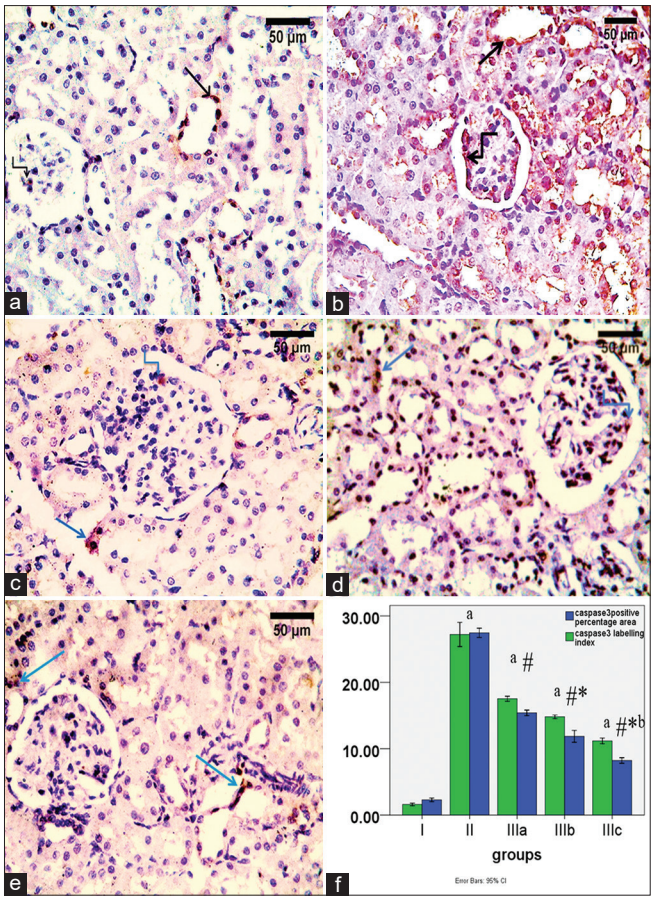

Figure 4: Photomicrographs of kidney sections. (a) The control showing few positive cells in renal tubules and renal corpuscles (b) Group II showing increased positive cells in renal tubules and corpuscles compared to control. (c) Subgroup IIIa, (d) Subgroup IIIb and (e) Subgroup IIIc showing decreased positive cells compared to diabetic rats. Positive cells in renal tubules (arrow) and renal corpuscles (stepwise arrow) (Caspase-3 immunostain, ×400, Scale bar = 50 μm) (f) Histogram showing the mean of caspase-3 positive percentage area and labeling index in all groups. [a]Significant compared to control, #Significant compared to group II, *Significant compared to group IIIa, b: Significant compared to group IIIb

CD68 antibody

Cytoplasmic immunoexpression of CD68 was detected in positive cells. The control group showed a few number of CD68-positive cells in between renal tubules. Group II showed numerous CD68 positive cells being demonstrated in renal corpuscles and renal tubules with a significant increase in the number of CD68 positive cells versus control. In all group III subgroups, showed less CD68 positive cells in renal corpuscles and renal tubules which were significantly decreased versus group II. Subgroups IIIb and IIIc showed a significant decrease than IIIa. Furthermore, subgroup IIIc significantly decreased than Subgroup IIIb [Figure 5 and Table 2].

Toluidine blue stain

The control group [Figure 6a] showed renal corpuscle containing renal glomeruli and surrounded by Bowman's capsule. Bowman's capsule had a parietal layer formed of simple squamous epithelium and a visceral layer containing podocytes. The PT had narrow lumen lined with cuboidal cells having rounded vesicular nuclei and apical brush borders. The DT had a wide lumen lined with cuboidal cells having rounded vesicular nuclei and no brush borders. Group II [Figure 6b and c] showed dilatation of urinary space and thickened basement membrane of renal corpuscle compared to the control rats. The nuclei of podocytes appeared irregular and deeply stained. Congested glomerular capillaries were observed. The cells lining renal tubules showed dense pyknotic nuclei, vacuolated cytoplasm. PT lost brush borders.

All group III subgroups [Figure 6d-f] revealed a narrower urinary space and decrease in the congestion of glomerular capillaries compared to diabetic rats. PT showed partially regular brush borders. Cells of proximal and DTs were less vacuolated compared to diabetic rats with subgroup IIIc [Figure 6f] sections were more or less similar to the control apart from few vacuoles in DTs.

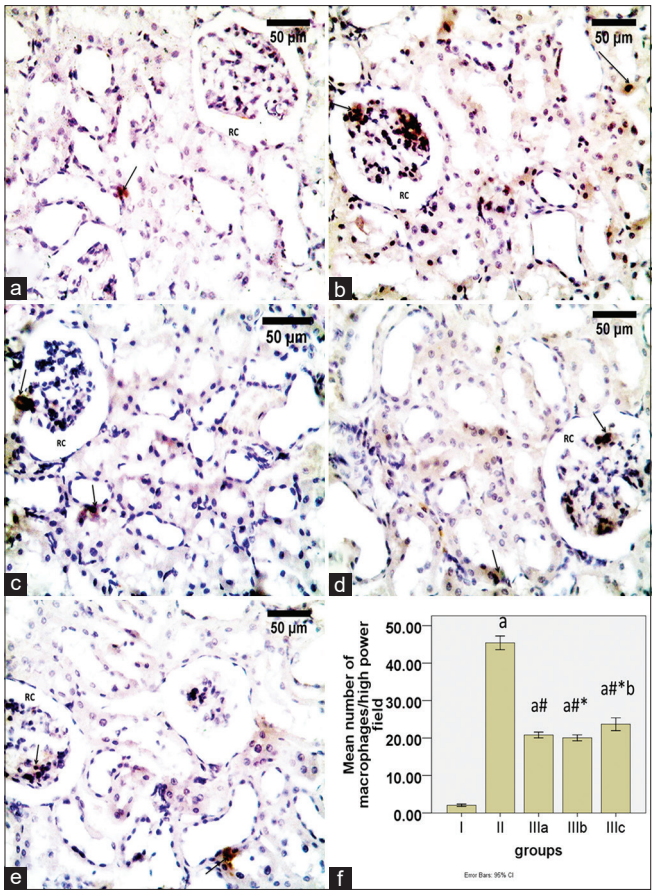

Figure 5: Photomicrographs of kidney sections. (a) Control showing few positive cells in between renal tubules and renal corpuscles (b) Group II showing increased positive cells in between renal tubules and renal corpuscles compared to control. (c) Subgroup IIIa, (d) Subgroup IIIb and (e) Subgroup IIIc: Showing decreased positive cells compared to diabetic rats. RC, positive cells in (arrow) (CD68 immunostain, ×400, Scale bar = 50 μm). (f) Histogram showing the mean number of CD68 positive cells in all groups. aSignificant compared to control, #Significant compared to group II, *Significant compared to group IIIa, b: Significant compared to group IIIb. RC: Renal corpuscle

Ultrastructural findings

In ultrathin sections of control rats, fenestrated endothelial cells with basal lamina were lining the glomerular capillaries. Podocytes were present surrounding the glomerular capillaries and exhibited long processes and small secondary foot processes. The secondary processes were closely related to endothelial cells of the glomerular capillaries forming the filtration barrier. GBM appeared with regular thickness [Figure 7].

The cells of PT were cuboidal in shape with euchromatic nucleus and numerous microvilli (MV). The basal parts showed longitudinally arranged mitochondria with basal infoldings [Figure 8a].

The cells of DT were cuboidal in shape with a euchromatic nucleus with few short apical MV. Mitochondria were longitudinally arranged with basal infoldings [Figure 8b].

Group II showed irregularly thickened GBM. The podocyte effacement appeared as retracted, widened, and shortened foot processes [Figure 9].

The cells lining PT showed absent MV with ill-defined basal infoldings. Mitochondria were swollen with homogeneous matrix and destructed cristae. The cytoplasm also contained numerous vacuoles and large lysosomes. The nucleus appeared heterochromatic with indentation [Figure 10a]. The cells of DT showed cytoplasmic vacuoles [Figure 10b].

All group III subgroups revealed less thickened GBM and effacement of foot processes of podocyte was reduced compared to diabetic group, as in [Figure 11] which demonstrating subgroup IIIa.

In subgroups IIIa, Cells of proximal tubule had regular euchromatic nuclei with less vacuoles and partially regular microvilli and mitochondria of different sizes and shapes in between irregular basal infolding [Figure 12a]. The cells lining distal tubule in subgroup IIIa appeared less vacuolated compared to those of diabetic group [Figure 12b]. In subgroup IIIb, less thickened GBM was observed and effacement of foot processes of podocyte was reduced compared to diabetic group [Figure 13]. Cells of proximal tubule had regular euchromatic nuclei with less vacuoles and partially regular microvilli and mitochondria of different sizes and shapes in between irregular basal infolding [Figure 14a].Cells of distal tubule had euchromatic nuclei, elongated basal mitochondria and few vacuoles compared to that in diabetic rats [Figure 14b]. Subgroup IIIc revealed less thickened GBM and effacement of foot processes of podocyte was reduced compared to diabetic group [Figure 15]. Subgroup IIIc showed that the cells of proximal tubules were more or less similar to control. Regular microvilli with longitudinally arranged mitochondria in between well defined basal infolding [Figure 16a and b]. Subgroup IIIc showed that the cells of distal tubule were more or less similar to control [Figure 16c].

Discussion

DN is a chronic kidney damage resulting from DM. EP and ginger are common medical herbs. EP attenuated diabetic nephrotoxicity in rat model due to its antioxidative effect.[8] The ameliorative effect of ginger was also previously reported on hyperglycemia-induced oxidative stress and inflammation.[15]

In the present study, we compared the possible effect of both EP and ginger, either alone or in combination on experimentally induced DN.

We observed that the kidney of diabetic rats showed widening of the urinary space, congestion of glomerular capillaries, and mesangial expansion. Renal tubules showed degenerative changes and dilatation. Similar changes associated with diabetes were previously reported.[30] These changes could be explained by oxidative damage induced by hyperglycemia with decreased glutathione antioxidant levels and increased lipid peroxidation products.[31]

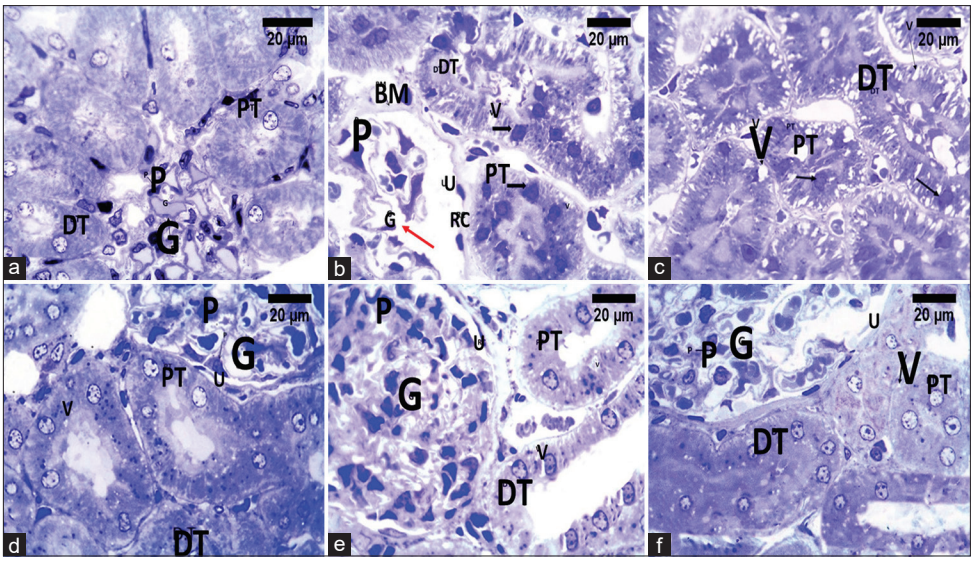

Figure 6: Photomicrographs of kidney semithin sections. (a) Control. showing glomeruli (G) lined with endothelial cells and podocyte (P) in renal corpuscle. PT lining cells are cuboidal with vesicular nuclei and apical brush border. DT lining cells are cuboidal with vesicular nuclei and wide lumen. (b) Diabetic rats showing; thickened (BM) widely spaced glomeruli (red arrow), congested glomerular capillaries (G) irregular and deeply stained nuclei (black arrow) of podocyte (P), widening of urinary space (U), PT loss of brush border. DTs vacuoles (V). (c) Diabetic rats showing; PT and DTs cells with irregular and deeply stained nuclei (black arrow) and numerous vacuoles (V). (d) Subgroup IIIa, (e) Subgroup IIIb and (f) Subgroup IIIc: Showing decreased degenerative changes; decreased congestion in glomerular capillaries (G) and narrower urinary space (U) with more regular nucleus of podocyte (P) compared to diabetic rats. PT appear with regular lumen and partially regular brush border and in f more or less similar to control. DT appear more or less similar to the control apart from few vacuoles (V) (Toluidine blue, ×1000, scale bar = 20 µm). PT: Proximal tubules, DT: Distal tubules, P: Podocyte, V: Vacuoles, G: Glomerular capillaries, U: Urinary space, RC: Renal corpuscle

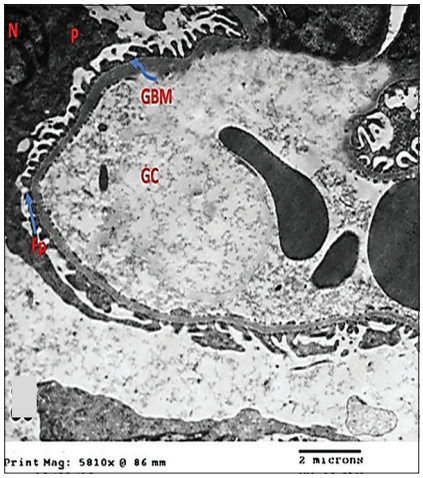

Figure 7: Electronmicrograph of ultrathin section in control group showing: GC with regular GBM (arrow curved) and podocyte (P) with Fp (arrow) surrounding GBM. Nucleus (N) of podocyte (TEM, ×5800, Scale bar = 2 µm). GC: Glomerular capillary, GBM: Glomerular basement membrane, Fp: Foot processes, N: Nucleus, P: Podocyte

In the current work, renal tubular cells of diabetic rats showed ultrastructural apoptotic features as pyknotic nuclei, numerous lysosomes, and vacuoles with loss of MV of PT. These results are in agreement with Matboli *et al*.[32] Cytoplasmic vacuoles may be lipid vacuoles, degenerated organelles, or autophagic vacuoles.[33]

Oxidative stress triggers the apoptotic cascade through mitochondrial release of cytochrome c, then cleavage and activation of cytoplasmic enzymes; caspases.[34] That was confirmed in our study by immunohistochemistry. A significant increase in active caspase 3 expression was observed in the diabetic group which was seen in tubular and glomerular cells. In line with our results, a previous study reported that endothelial cells, tubulointerstitial cells, podocytes, and mesangial cells can undergo apoptosis in DN.[35]

Podocytes effacement was an important ultrastructure feature observed in our study. Previous studies are in agreement with our results.[33,36] Mundel and Shankland[36] explained that this could be due to changes in slit diaphragm proteins, podocyte and GBM interactions, cytoskeleton, or negative apical membrane of podocytes.

In the current study, an increase in thickness of GBM with PAS stain and ultrastructurally was detected in diabetic rats. These findings are in agreement with previous studies.[33,37-40] That could be due to that hyperglycemia induces hyperfiltration and hyperperfusion, which cause mechanical stretching with excess production of extracellular matrix.[41] Increased extracellular matrix production and decreased proteoglycans charge density lead to proteinuria and glomerular sclerosis.

In our study, the diabetic group exhibited a significant increase in collagen fibers with interstitial fibrosis as another consequence of extracellular matrix accumulation. This might be due to inflammatory response and cellular degeneration associated with persistent hyperglycemia.[42] Similar findings were reported by previous studies[24,39]

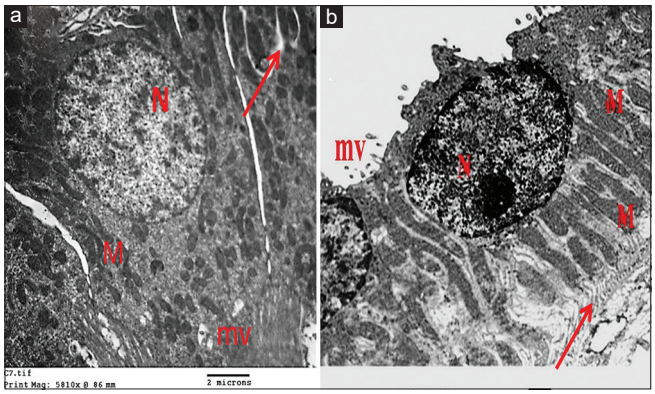

Figure 8: Electronmicrographs of ultrathin sections in the control group showing: (a) Proximal tubular cells with numerous apical MV, basal infoldings (arrow) in which the elongated mitochondria (M) arranged with large rounded and euchromatic nucleus (N). (b) Distal tubular cells with a euchromatic nucleus (N), basal infoldings (arrow) and elongated mitochondria (M) (TEM, ×5800, Scale bar = 2 μm). MV: Microvilli, M: Mitochondria, N: Nucleus

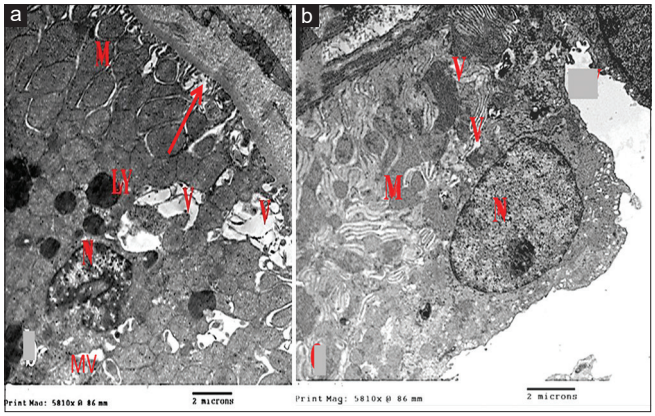

Figure 10: Electronmicrographs of ultrathin sections of diabetic rats showing: (a) Proximal tubular cells with heterochromatic nucleus and nuclear indentation (N) and ill-defined basal infoldings (arrow) with mitochondria of different sizes and shapes (M). Destructed MV. The cytoplasm shows LY and numerous vacuoles (V). (b) Distal tubular cell with vacuoles (V), Mitochondria with mitochondria of different sizes and shapes (M), nucleus (N) (TEM, ×5800, Scale bar = 2 μm). MV: Microvilli, LY: Lysosomes, M: Mitochondria, N: Nucleus, V: Vacuoles

Our immunohistochemical results revealed a significant increase in CD68-positive cell number. Previous studies are in accordance with our results.[43,44] It was proved that macrophages accumulation in the interstitium was associated with albuminuria and renal function loss while macrophage accumulation in glomeruli was associated with the degree of glomerular sclerosis.[44]

This might be due to the inflammatory response associated with persistent hyperglycemia. Endoplasmic reticulum stress and intracellular signal transduction pathways activate inflammatory factors.[42]

In addition, macrophages produce proinflammatory cytokines that induce inflammatory response and apoptosis in target

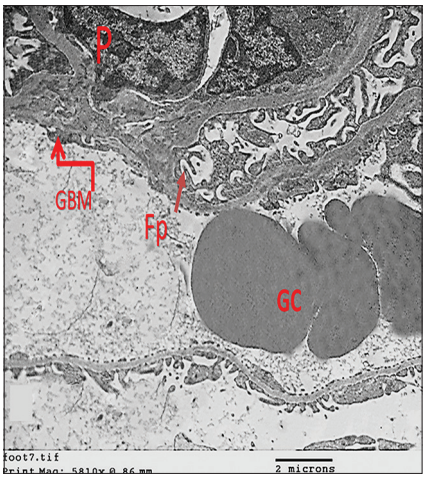

Figure 9: Electronmicrograph of ultrathin section of diabetic rats showing GC with irregular thickening of GBM (arrow curved) and effacement of Fp (arrow) of podocytes (P) (TEM, ×5800, Scale bar = 2 μm). GC: Glomerular capillaries, GBM: Glomerular basement membrane, Fp: foot processes, P: Podocytes

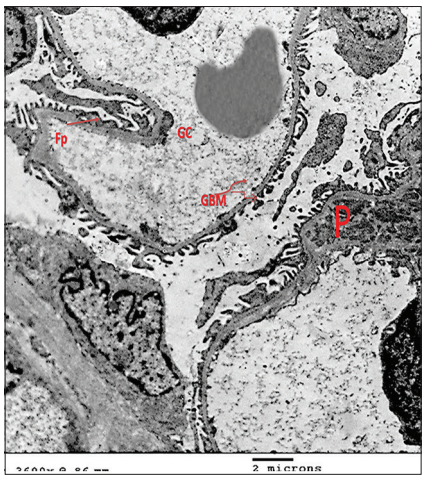

Figure 11: Electron micrograph of ultrathin section of subgroup IIIa showing: GC with less thickened glomerular basement membrane (GBM curved arrow) and less effacement of Fp (arrow) of podocytes (P) compared to diabetic rats (TEM, ×5800, Scale bar = 2 μm). GC: Glomerular capillary, Fp: Foot processes, P: Podocytes, GBM: Glomerular basement membrane

cells,[45] and promote insulin resistance. They activate the N-terminal kinase and the nuclear factor-kappa B pathways which interfere with insulin signaling in peripheral tissues.[46] Likewise, macrophage infiltration was observed in liver, muscles, adipose tissue, and pancreas of diabetic models.[47]

In the present study, subgroup IIIa showed partial improvement in renal changes such as decreased degenerative changes. A significant decrease in caspase 3 expression area percentage and LI, PAS reaction, and collagen area percentage were observed with comparison to group II. Ultrastructurally, a regular thickness of GBM and attenuation of effacement with decreased apoptotic features were seen.

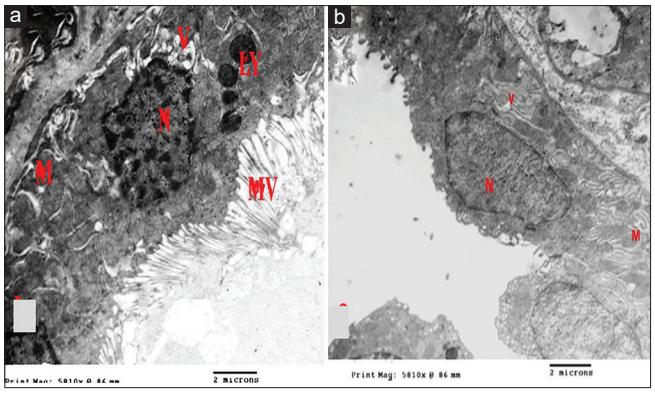

Figure 12: Electron micrographs of ultrathin sections of subgroup IIIa showing: (a) proximal tubular cell with partially regular apical microvilli (MV) and basal mitochondria of different sizes and shapes(M) in between irregular infoldings. The nucleus (N) appears more regular and the cytoplasm shows less vacuoles (V) and lysosomes (Ly) compared to diabetic rats. (b) distal tubular cells with less vacuoles (V) compared to diabetic rats. Note regular nucleus (N), basal mitochondria (M). (TEM x5800, Scale bar=2μm)

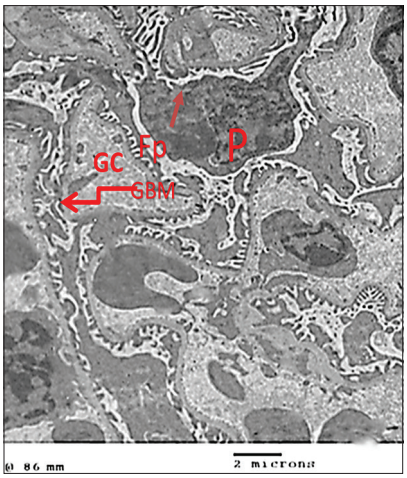

Figure 13: electron micrograph of ultrathin section in subgroup IIIb showing: glomerular capillaries (GC) with less thickened glomerular basement membrane (GBM curved arrow) compared to group IIIa with footprocesses (Fp arrow) of podocytes (P). (TEM x5800, Scale bar=2μm)

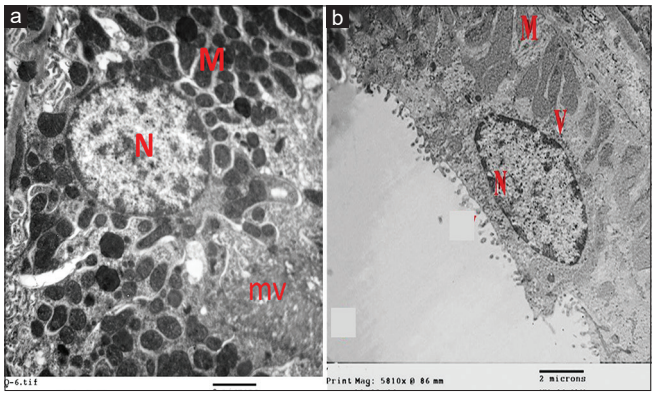

Figure 14: Electron micrographs of ultrathin sections of subgroup IIIb (a) proximal tubular cell with partially regular apical microvilli (mv), euchromatic nucleus (N) with basal mitochondria (M) of different shapes in between well defined basal infoldings. The cytoplasm shows less vacuoles compared to diabetic rats. (b) distal tubular cell with euchromatic nucleus (N), basal mitochondria (M) and few vacuoles (V). (TEM x5800, Scale bar=2μm)

Figure 15: Electron micrograph of ultrathin section in subgroup IIIc showing regular glomerular basement membrane (GBM curved arrow) and foot processes (Fp arrow) of podocytes (P) that are more or less similar to control group, glomerular capillaries (GC). (TEM x5800. Scale bar=2μm)

In accordance with our findings, Mao *et al.*[6] reported that EP provided a protective effect on testis of diabetic rats. They reported that *Echinacea* prevents lipid peroxidation, oxidative stress, and insulin resistance. It inhibits nitric oxide production.[48]

Similarly, Shi *et al.*[49] found that EP caused a significant decrease in PAS intensity in kidneys of mice treated with lipopolysaccharide. In addition, it was reported that EP reduced collagen fibers accumulation in magnetic nanoparticles-induced testicular toxicity[50] and decreased apoptosis in the spleen of diabetic rats.[28] Moreover, Bayramoğlu *et al.*[17] reported that *Echinacea* improved tubular degeneration in ischemia/reperfusion injury in rats.

Regarding the anti-inflammatory role of EP, a significant decrease in the number of macrophages was detected in subgroup IIIa versus group II. Similarly, EP induced a significantly decreased inflammatory cytokines produced by macrophages; TNF-α and IL-1β, in the testis of diabetic rats.[6]

In the current study, subgroup IIIb exhibited a more prominent improvement of diabetic-induced degenerative changes than EP. We found a significantly reduced PAS reaction, percentage of collagen area, and caspase-3 expression versus both group II and subgroup IIIa.

Similar results were reported in previous studies.[51,52] This could be attributed to the hypoglycemic effect of ginger.[53] In addition, flavonoids (one of the ginger constituents) can improve the oxidative stress that causes impairment of pancreatic beta cell function.[54] Shirpoor *et al.*[55] also found that ginger decreased collagen accumulation in rats treated with ethanol. An antiapoptotic role of ginger was also reported in previous studies.[56-58]

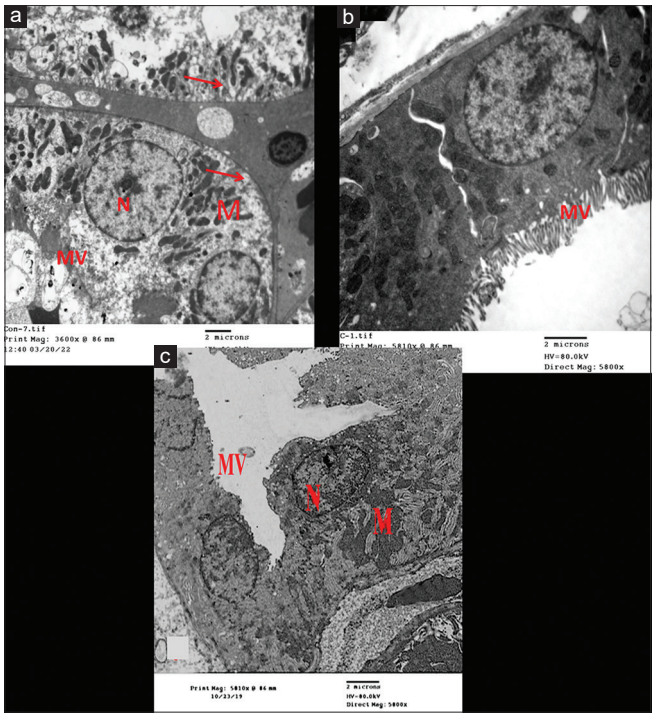

Figure 16: Electron micrographs of ultrathin sections in subgroup IIIc showing (a): Proximal tubular cell with euchromatic nucleus (N) with longitudinally arranged mitochondria (M) with regular well-defined basal infolding (arrow) MV (TEM, ×3600). (b) Proximal tubular cell with regular well-defined MV (c) Distal tubular cells with a euchromatic nucleus (N), basal infoldings with longitudinally arranged mitochondria (M), MV (TEM, ×5800. Scale bar = 2 μm). MV: Microvilli, N: Nucleus

In the current study, ginger significantly decreased the number of macrophages versus that in the diabetic animals. Similar results were reported in kidney,[59] spleen,[60] and in an experimental model colitis.[61] Arablou *et al.*[60] reported that ginger decreased inflammatory markers in diabetic patients.

We observed that the number of macrophages significantly decreased with ginger versus EP and that could be attributed to the hypoglycemic effect,[52] in addition to the antioxidant effect exhibited by ginger.[62] Sultana *et al.*[53] explained that ginger can antagonize suppression of insulin release induced through serotonin receptors. Previous studies reported that ginger has an inhibitory effect on the glycolytic activity of brush border enzymes in enterocytes.[54]

In our study, subgroup IIIc revealed more prominent improvement in renal degenerative and fibrotic changes induced by diabetes with significantly decreased caspase expression and number of macrophages compared to subgroups IIIa, IIIb.

Conclusion

Finally, it is concluded that ginger either single or combined with EP could have a more significant protective role than EP alone in DN model. They can be used as an adjuvant treatment to minimize renal complications associated with diabetes.

Abbreviations

DN; Diabetic nephropathy, STZ; streptozotocin (STZ), DM; diabetes mellitus, EP; *Echinacea purpurea*, DKD; diabetic kidney disease.

Financial support and sponsorship

Nil.

Conflicts of interest

There are no conflicts of interest.

References

1. Ogunyinka BI, Oyinloye BE, Osunsanmi FO, Opoku AR, Kappo AP. Protective effects of *Parkia biglobosa* protein isolate on streptozotocin-induced hepatic damage and oxidative stress in diabetic male rats. Molecules 2017;22:1654.
2. Giralt-López A, Molina-Van den Bosch M, Vergara A, García-Carro C, Seron D, Jacobs-Cachá C, *et al.* Revisiting experimental models of diabetic nephropathy. Int J Mol Sci 2020;21:3587.
3. Valencia WM, Florez H. How to prevent the microvascular complications of type 2 diabetes beyond glucose control. BMJ 2017;356:i6505.
4. Samsu N. Diabetic nephropathy: Challenges in pathogenesis, diagnosis, and treatment. Biomed Res Int 2021;2021:17. https://doi.org/10.1155/2021/1497449.
5. Faridi Esfanjani A, Jafari SM. Biopolymer nano-particles and natural nano-carriers for nano-encapsulation of phenolic compounds. Colloids Surf B Biointerfaces 2016;146:532-43.
6. Mao CF, Zhang XR, Johnson A, He JL, Kong ZL. Modulation of diabetes mellitus-induced male rat reproductive dysfunction with micro-nanoencapsulated *Echinacea purpurea* ethanol extract. Biomed Res Int 2018;2018:1-17.
7. Mao CF, Sudirman S, Lee CC, Tsou D, Kong ZL. *Echinacea purpurea* ethanol extract improves male reproductive dysfunction with streptozotocin-nicotinamide-induced diabetic rats. Front Vet Sci 2021;8:651286.
8. Mohammedsaleh ZM, Aljadani HM. *Echinacea purpurea* root extract modulates diabetes-induced renal dysfunction in rats through hypoglycemic, antioxidants, and anti. Science 2021;25:1033-43.
9. Attokaran, M. Ginger. in Natural Food Flavors and Colorants. Second ed Wiley-Blackwell. Hoboken, New Jersey. chapter 2017;57:209-14.
10. Therkleson T. Topical ginger treatment with a compress or patch for osteoarthritis symptoms. J Holist Nurs 2014;32:173-82.
11. Lai YS, Lee WC, Lin YE, Ho CT, Lu KH, Lin SH, *et al.* Ginger essential oil ameliorates hepatic injury and lipid accumulation in high fat diet-induced nonalcoholic fatty liver disease. J Agric Food Chem 2016;64:2062-71.
12. Panahi Y, Saadat A, Sahebkar A, Hashemian F, Taghikhani M, Abolhasani E. Effect of ginger on acute and delayed chemotherapy-induced nausea and vomiting: A pilot, randomized, open-label clinical trial. Integr Cancer Ther 2012;11:204-11.
13. Daily JW, Zhang X, Kim DS, Park S. Efficacy of ginger for alleviating the symptoms of primary dysmenorrhea: A systematic review and meta-analysis of randomized clinical trials. Pain Med 2015;16:2243-55.
14. Wang J, Ke W, Bao R, Hu X, Chen F. Beneficial effects of ginger *Zingiber officinale* Roscoe on obesity and metabolic syndrome: A review. Ann N Y Acad Sci 2017;1398:83-98.
15. Al Hroob AM, Abukhalil MH, Alghonmeen RD, Mahmoud AM. Ginger alleviates hyperglycemia-induced oxidative stress, inflammation and apoptosis and protects rats against diabetic nephropathy. Biomed Pharmacother 2018;106:381-9.
16. Khalaf AA, Hussein S, Tohamy AF, Marouf S, Yassa HD, Zaki AR, *et al.* Protective effect of *Echinacea purpurea* (Immulant) against cisplatin-induced immunotoxicity in rats. Daru 2019;27:233-41.
17. Bayramoğlu G, Kabay Ş, Özden H, Üstüner MC, Uysal O, Bayramoğlu A, *et al*. The effect of Echinacea on kidney and liver after experimental renal ischemia/reperfusion injury in the rats. Afr J Pharm Pharmacol 2011;5:1561-6.

18. El-Kott AF, El-Sayad SM, Abdel-Aziz AM. The effects of ginger (*Zingiber officinale*) on histology and immunohistochemistry of liver and kidney and certain haematological parameters in alloxan induced diabetic rats. Egypt J Exp Biol (zool) 2010;6:61-70.
19. Bancroft JD, Gamble M. Theory and practice of histological techniques. 6th Edition, Churchill Livingstone, Elsevier, China: Elsevier health sciences; 2008.
20. Pereira T, Naik S, Tamgadge A. Quantitative evaluation of macrophage expression using CD68 in oral submucous fibrosis: An immunohistochemical study. Ann Med Health Sci Res 2015;5:435-41.
21. Miura M, Chen XD, Allen MR, Bi Y, Gronthos S, Seo BM, *et al.* A crucial role of caspase-3 in osteogenic differentiation of bone marrow stromal stem cells. J Clin Invest 2004;114:1704-13.
22. Nambiar S, Haragannavar VC, Augustine D, Sowmya S, Rao RS, Kumari K, *et al*. Immunohistochemistry: A brief review. J Dent Orofac Res 2016;12:25-9.
23. Lavres J Jr., Reis AR, Rossi ML, Cabral CP, Nogueira ND, Malavolta E. Changes in the ultrastructure of soybean cultivars in response to manganese supply in solution culture. Sci Agricol 2010;67:287-94.
24. Yang X, Han X, Wen Q, Qiu X, Deng H, Chen Q. Protective effect of keluoxin against diabetic nephropathy in type 2 diabetic mellitus models. Evid Based Complement Alternat Med 2021;2021:e 8455709. doi: 10.1155/2021/8455709.
25. Bohuslavova R, Cerychova R, Nepomucka K, Pavlinkova G. Renal injury is accelerated by global hypoxia-inducible factor 1 alpha deficiency in a mouse model of STZ-induced diabetes. BMC Endocr Disord 2017;17:48.
26. Palmer MB, Vichot AA, Cantley LG, Moeckel GW. Quantification and localization of M2 macrophages in human kidneys with acute tubular injury. Int J Nephrol Renovasc Dis 2014;7:415-9.
27. Ismail DI, Aboulkhair AG. The effect of aliskiren on renal cortical ischemia/reperfusion injury in albino rats: A histological and immunohistochemical study. Egypt J Histol 2019;42:838-48.
28. Said HM, Abdelaziz HO, Abd Elhaliem NG, Elsherif SA. A comparative study between ginger and echinacea possible effect on the albino rat spleen of experimentally induced diabetes. Egypt J Histol 2020;43:763-76.
29. Bryman A, Cramer D. Quantitative Data Analysis with SPSS 14, 15 & 16: A Guide for Social Scientists. Quantitative Data Analysis With SPSS 14, 15 & 16: A Guide for Social Scientists. New York, NY, US: Routledge/Taylor & Francis Group; 2009. p. xxv, 381-xxv, 381.
30. Aldahmash BA, El-Nagar DM, Ibrahim KE, Metwaly MS. Biotin amelioration of nephrotoxicity in streptozotocin-induced diabetic mice. Saudi J Biol Sci 2015;22:564-9.
31. Onk D, Onk OA, Erol HS, Özkaraca M, Çomaklı S, Ayazoğlu TA, *et al.* Effect of melatonin on antioxidant capacity, ınflammation and apoptotic cell death in lung tissue of diabetic rats. Acta Cir Bras 2018;33:375-85.
32. Matboli M, Eissa S, Ibrahim D, Hegazy MG, Imam SS, Habib EK. Caffeic acid attenuates diabetic kidney disease via modulation of autophagy in a high-fat diet/streptozotocin-induced diabetic rat. Sci Rep 2017;7:2263.
33. Ebrahim N, Ahmed IA, Hussien NI, Dessouky AA, Farid AS, Elshazly AM, *et al.* Mesenchymal stem cell-derived exosomes ameliorated diabetic nephropathy by autophagy induction through the mTOR signaling pathway. Cells 2018;7:E226.
34. Chen M, Wang J. Initiator caspases in apoptosis signaling pathways. Apoptosis 2002;7:313-9.
35. Pourghasem M, Shafi H, Babazadeh Z. Histological changes of kidney in diabetic nephropathy. Caspian J Intern Med 2015;6:120-7.
36. Mundel P, Shankland SJ. Podocyte biology and response to injury. J Am Soc Nephrol 2002;13:3005-15.
37. Kumar GS, Shetty AK, Salimath PV. Modulatory effect of bitter gourd (Momordica charantia LINN.) on alterations in kidney heparan sulfate in streptozotocin-induced diabetic rats. J Ethnopharmacol 2008;115:276-83.
38. Dong Z, Sun Y, Wei G, Li S, Zhao Z. Ergosterol ameliorates diabetic nephropathy by attenuating mesangial cell proliferation and extracellular matrix deposition via the TGF-β1/Smad2 signaling pathway. Nutrients 2019;11:E483.
39. Xu S, He L, Ding K, Zhang L, Xu X, Wang S, *et al.* Tanshinone IIA ameliorates streptozotocin-induced diabetic nephropathy, partly by attenuating perk pathway-induced fibrosis. Drug Des Devel Ther 2020;14:5773-82.
40. Harada S, Ushigome H, Nishimura A, Nakao T, Nakamura T, Koshino K, *et al.* Histological reversibility of diabetic nephropathy after kidney transplantation from diabetic donor to non-diabetic recipient. Nephrology (Carlton) 2015;20 Suppl 2:40-4.
41. Uil M, Scantlebery AM, Butter LM, Larsen PW, de Boer OJ, Leemans JC, *et al.* Combining streptozotocin and unilateral nephrectomy is an effective method for inducing experimental diabetic nephropathy in the 'resistant' C57Bl/6J mouse strain. Sci Rep 2018;8:5542.
42. Faustino VD, Arias SC, Ferreira Ávila V, Foresto-Neto O, Zambom FFF, Machado FG, *et al.* Simultaneous activation of innate and adaptive immunity participates in the development of renal injury in a model of heavy proteinuria. Biosci Rep 2018;38:BSR20180762.
43. Zhang P, Sun Y, Peng R, Chen W, Fu X, Zhang L, *et al.* Long non-coding RNA Rpph 1 promotes inflammation and proliferation of mesangial cells in diabetic nephropathy via an interaction with Gal-3. Cell Death Dis 2019;10:526.
44. Lim AK, Tesch GH. Inflammation in diabetic nephropathy. Mediators Inflamm 2012;2012:146154.
45. Ma T, Li X, Zhu Y, Yu S, Liu T, Zhang X, *et al.* Excessive activation of notch signaling in macrophages promote kidney inflammation, fibrosis, and necroptosis. Front Immunol 2022;13:835879.
46. Esser N, Legrand-Poels S, Piette J, Scheen AJ, Paquot N. Inflammation as a link between obesity, metabolic syndrome and type 2 diabetes. Diabetes Res Clin Pract 2014;105:141-50.
47. Eguchi K, Manabe I. Macrophages and islet inflammation in type 2 diabetes. Diabetes Obes Metab 2013;15 Suppl 3:152-8.
48. Rezaie A, Fazlara A, Haghi Karamolah M, Shahriari A, Najaf Zadeh H, Pashmforosh M. Effects of *Echinacea purpurea* on hepatic and renal toxicity induced by diethylnitrosamine in rats. Jundishapur J Nat Pharm Prod 2013;8:60-4.
49. Shi Q, Lang W, Wang S, Li G, Bai X, Yan X, *et al.* Echinacea polysaccharide attenuates lipopolysaccharide-induced acute kidney injury via inhibiting inflammation, oxidative stress and the MAPK signaling pathway. Int J Mol Med 2021;47:243-55.
50. Awaad A, Adly MA, Hosny D. Histological and histopathological studies on the protective role of *Echinacea purpurea* extract after intra-testicular injection of magnetic nanoparticles in male albino rats. J Histotechnol 2017;40:100-114.
51. Al-Qudah MM., Al-Ramamneh MA, Al-Abbadi A, Al-Salt J. The histological effect of aqueous ginger extract on kidneys and lungs of diabetic rats. Int J Biol 2018;10:23-8.
52. Payami S-A, Babaahmadi-Rezaei H, Ghaffari M-A, Mansouri E, Mohammadzadeh G. Hydroalcoholic extract of *Zingiber officinale* improves stz-induced diabetic nephropathy in rats by reduction of nf-κb activation. Jundishapur J Nat Pharm Prod 2019;14:e55063. doi: 10.5812/jjnpp.55063.
53. Sultana S, Khan MI, Rahman H, Nurunnabi AS, Afroz RD. Effects of ginger juice on blood glucose in alloxan induced diabetes mellitus in rats. J Dhaka Med Coll 2014;23:14-7.
54. Shanmugam KR, Mallikarjuna K, Kesireddy N, Sathyavelu Reddy K. Neuroprotective effect of ginger on anti-oxidant enzymes in streptozotocin-induced diabetic rats. Food Chem Toxicol 2011;49:893-7.
55. Shirpoor A, Gharalari FH, Rasmi Y, Heshmati E. Ginger extract attenuates ethanol-induced pulmonary histological changes and oxidative stress in rats. J Biomed Res 2017;31:521-7.
56. Hajhosieni L, Rostami FF, Khaki A. Bioflavonoids effects of ginger on glomerular podocyte apoptosis in streptozotocin-induced diabetic rat. Crescent J Med Biol Sci 2014;1:42-5.
57. Moawad AA, Abo Baker SH. Histological assessment of ginger (*Zingiber officinale*) extract on tongue dorsal surface in diabetic rats. Egypt Dent J (2-April (Oral Med, X-Ray, Oral Biol & Oral Pathol)) 2020;66:991-6.
58. Yi JK, Ryoo ZY, Ha JJ, Oh DY, Kim MO, Kim SH. Beneficial effects of 6-shogaol on hyperglycemia, islet morphology and apoptosis in some tissues of streptozotocin-induced diabetic mice. Diabetol Metab Syndr 2019;11:15.
59. Yang M, Liu C, Jiang J, Zuo G, Lin X, Yamahara J, *et al.* Ginger extract

diminishes chronic fructose consumption-induced kidney injury through suppression of renal overexpression of proinflammatory cytokines in rats. BMC Complement Altern Med 2014;14:174.
60. Arablou T, Aryaeian N, Valizadeh M, Sharifi F, Hosseini A, Djalali M. The effect of ginger consumption on glycemic status, lipid profile and some inflammatory markers in patients with type 2 diabetes mellitus. Int J Food Sci Nutr 2014;65:515-20.
61. Zhou X, Liu X, He Q, Wang M, Lu H, You Y, *et al.* Ginger extract decreases susceptibility to dextran sulfate sodium-induced colitis in mice following early antibiotic exposure. Front Med (Lausanne) 2021;8:1-14.
62. Essawy AE, Abdel-Wahab WM, Sadek IA, Khamis OM. Dual protective effect of ginger and rosemary extracts against CCl_4-induced hepatotoxicity in rats. Environ Sci Pollut Res Int 2018;25:19510-7.